Experimental investigation on the spray characteristics of agricultural full-cone pressure swirl nozzle

Xiuyun Xue[1,2,3,4], Xufeng Xu[1], Shilei Lyu[1,2], Shuran Song[1,2,3], Xin Ai[1], Nengchao Li[1], Zhenyu Yang[1], Zhen Li[1,2,3,4*]

(1. *College of Electronic Engineering (College of Artificial Intelligence), South China Agricultural University, Guangzhou 510642, China*;
2. *National Citrus Industry Technical System Machinery Research Office, Guangzhou 510642, China*;
3. *Engineering Research Center for Monitoring Agricultural Information of Guangdong Province, Guangzhou 510642, China*;
4. *Meizhou SCAU-Zhensheng Research Institute for Modern Agricultural Equipment, Meizhou 514781, China*)

Abstract: The spray characteristics of a full-cone pressure swirl nozzle have been investigated in this study. The results were defined by Reynolds number, which focuses on the breakup of liquid film, droplet size, velocity, and liquid volume flux under different Reynolds numbers at the near-field spray. The spray structure was visualized using a high-speed camera, and the characteristics of droplets were measured using a Phase Doppler Anemometer (PDA) in both the radial and axial directions. The tests were carried out at varying spray pressures (0.2 to 1.0 MPa), corresponding to different Reynolds numbers (5369 to 12 006). It was found that when the Reynolds number rises, the liquid became more unstable after leaving the nozzle, causing the liquid film to break up faster. According to the measurements of PDA, the coalescence of droplets increased due to the centrifugal effect. What's more, the velocity of the droplets fluctuates significantly in the radial direction, and the droplets with a smaller particle size had a higher average velocity. From the perspective of liquid distribution, the increase in Reynolds number caused the spray liquid to move in the radial direction gradually. In contrast, the liquid volume distribution changed in the radial direction more obviously than in the axial direction, growing to the maximum along the radial direction and gradually reducing. It can provide a reference for selecting operating parameters for actual agricultural spray operations and the design of electrostatic nozzles through the research on breakup and droplet characteristics.

Keywords: full-cone pressure swirl nozzle, droplet size, droplet velocity, liquid volume flux, high-speed camera, PDA
DOI: 10.25165/j.ijabe.20231604.7088

Citation: Xue X Y, Xu X F, Lyu S, Song S R, Ai X, Li N C, et al. Experimental investigation on the spray characteristics of agricultural full-cone pressure swirl nozzle. Int J Agric & Biol Eng, 2023; 16(4): 29–40.

1 Introduction

The pressure swirl nozzle is widely utilized in a variety of areas, including agricultural applications. The pressure swirl nozzle is one of the most commonly used nozzles in orchards and vineyards. It is possible to increase pesticide application efficiency by combining electrostatic atomization technology[1,2]. Pressure swirl nozzles are one of the many devices used to accomplish liquid disintegration. They may create well-atomized sprays by breaking up the liquid layer. With the high angular momentum obtained in the nozzle, the liquid film soon becomes unstable and disintegrates because of different mechanisms[3]. Full-cone nozzles, as opposed to fan and hollow-cone nozzles, can create a more uniform cross-section spray and provide more coverage[4,5].

Received date: 2021-09-28 **Accepted date:** 2022-11-07
Biographies: Xiuyun Xue, PhD, Associate Professor, research interest: crop protection and machinery engineering, Email: xuexiuyun@scau.edu.cn; **Xufeng Xu**, MS, research interest: spray technology, Email: 13422174883@163.com; **Shilei Lyu**, PhD, Associate Professor, research interest: intelligent detection and control, Email: lvshilei@scau.edu.cn; **Shuran Song**, PhD, Professor, research interest: crop protection and machinery engineering, Email: songshuran@scau.edu.cn; **Xin Ai**, MS, research interest: spray technology, Email: 1095990604@qq.com; **Nengchao Li**, MS, research interest: spray technology, Email: 2273404385@qq.com; **Zhenyu Yang**, MS, research interest: spray technology, Email: 448150135@qq.com.
***Corresponding author: Zhen Li**, PhD, Professor, research interest: orchard machinery and equipment. College of Electronic Engineering, South China Agricultural University, Guangzhou 510642, China. Tel: +86-20-85282269, Email: lizhen@scau.edu.cn.

The efficient deposition of pesticides on the target is determined by the characteristics of droplet size and velocity. Spray drift and other undesirable effects are caused by tiny droplet[6]. Large droplets will bounce back on the leaf surface, decreasing the amount of material deposited on the target[7,8]. The properties of droplet velocity, which are connected to the disintegration of liquid film and droplet size, are typically regarded as one of the most significant factors in evaluating the spray quality for pressure swirl nozzles. The liquid exiting the nozzle is more likely to travel from the spray axis to the spray perimeter at a higher tangential velocity, increasing spray dispersion and a broader spray angle. More dispersion in the full-cone spray nozzle means a more uniform circumferential distribution of liquid in the spray[9,10]. However, the droplet size and velocity characteristics are connected to the breakup of the liquid film and the collision, coalescence, and subsequent breakup of the droplets in the near field of the spray[11]. What's more, in terms of studying spray characteristics in the near field of the nozzle, electrostatic nozzles must establish the most appropriate charging position of the electrode and the electrode width. According to the electrostatic nozzle experiment of Patel et al., a distance of 2-3 mm between the electrode and the nozzle may achieve the optimum charge-to-mass ratio of 2.8 mC/kg, which is governed by the liquid film breakup length and nozzle design[12].

The spray properties of the pressure swirl nozzle have been the subject of the majority of investigations. Senecal et al.[13] used the liquid film-ligament-droplet hypothesis to correctly predict the process of liquid film breakup and droplet size in pressure swirl nozzles. Saha et al.[14] investigated the breakup characteristics of two

hydraulic injector nozzles using shadowgraph technology and PDPA. According to their conclusion, which analyzed by the characteristics of droplet diameters and velocities, the spray is subdivided into three zones: zone 1 is consisted of film and ligament with primary breakup and some secondary breakup; zone 2 continues to undergo secondary breakup, but the centrifugal dispersion becomes dominant; and zone 3 that away from the spray happens more coalescence of droplets. Davanlou et al.[15] conducted an experimental investigation of the breakup properties of liquids with various surface tensions and viscosities, as well as the droplet size during spraying. The findings revealed that surface tension and viscosity impact droplet behavior, as measured by droplet velocity and diameter distribution in axial and radial directions in terms of Reynolds number. When liquid leaves the nozzle, it condenses into the liquid film, which is unstable owing to the air's interaction. When liquid leaves the nozzle, it condenses into a liquid film, which is unstable owing to air contact. According to prior research, the instability in the sinusoidal model grows fast. Once the instability reaches its limit, the liquid film will break up. The breakup length of the liquid film plays a vital role in the atomization of ligaments and droplet characteristics, such as diameter, velocity, and spray cone angle. However, most studies on the liquid film breakup of pressure swirl nozzles concentrate more on hollow-cone nozzles than full-cone nozzles.

The main objectives of this research are to experimentally investigate the effect of Reynolds number on the spray characteristics including the breakup of the liquid film, droplet size, velocity, and liquid volume flux in a full-cone pressure swirl nozzle. The research consists of flow visualization using a high-speed camera and simultaneous droplet size, velocity, and liquid volume flux measurements with Phase Doppler Anemometry (PDA). In addition, liquid film breakup length and spray cone angle are quantified based on spray images captured by the high-speed camera. With the theory of liquid film breakup and the analysis of droplet characteristics in the axial and radial direction, the study will provide a complete description of the near-field spray.

2 Materials and methods

2.1 Experimental system

The experiment was conducted in an ambient room with a temperature of 25°C and relative humidity of 50%. The spray conducted in the experiment was mainly completed by the constant pressure spray system, as illustrated in Figure 1. The constant pressure spray system included a constant pressure controller, frequency converter, plunger pump, variable-frequency motor, pressure sensor, flowmeter, and the pressure swirl nozzle.

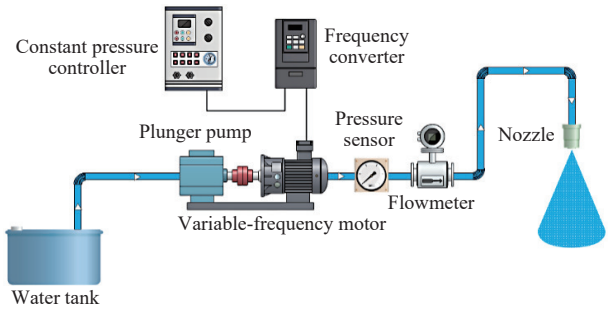

Figure 1 Constant pressure spray system

The system utilized the fuzzy PID algorithm to optimize spray pressure management in order to maintain a consistent pressure and reduce the experimental error. Figure 2 gives the principle of the spray system to achieve a constant spray pressure. Firstly, the spray pressure $U_r(k)$ was set through the input panel of the controller. The pressure sensor collected the spray pressure in real-time and converted the pressure signal into an electrical signal, which was converted into a feedback signal $U_c(k)$ by the signal conditioning circuit. After the fuzzy PID controller acquired $U_r(k)$ and $U_c(k)$, it calculated the $U_f(k)$ by adjusting the fuzzy PID algorithm online, and output $U_f(k)$ to the analog control terminal of the frequency converter to control the AC frequency. The change in frequency made the speed of the motor and the pump change to realize the constant pressure in the spray system. A two-dimensional fuzzy controller structure was used to output the PID parameter adjustment amount by inputting the pressure signal error and the change rate of the pressure signal error and then establishing fuzzy rules for fuzzy reasoning. Finally, the control increment was obtained by the PID controller so that the new control quantity was output[16]. The fuzzy PID control algorithm can make the system keep the spray pressure constant and reduce the experimental error.

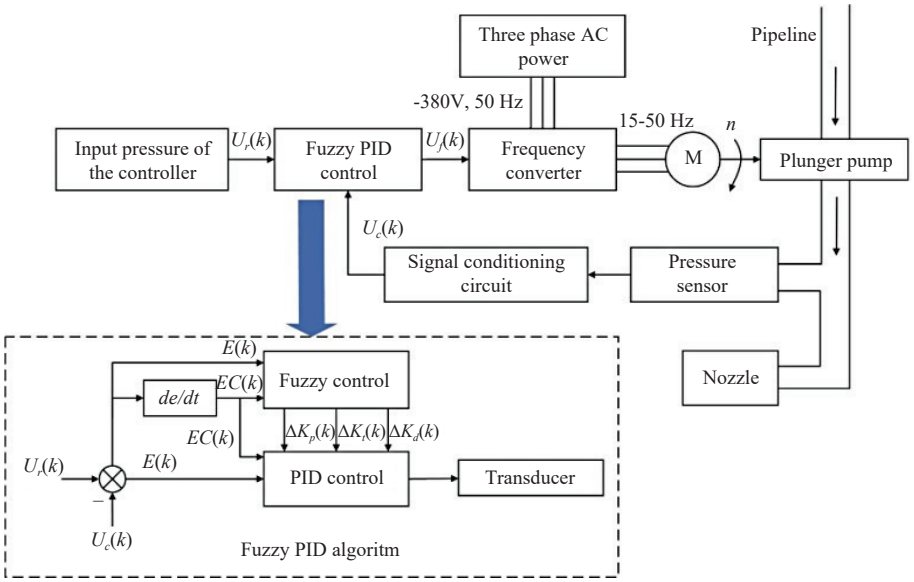

Figure 2 Principle of the spray system

The primary goal of the research is to study a full-cone pressure swirl nozzle (IKEUCHI Co., Japan). With X-shaped in the nozzle, the liquid is rotated and atomized from the nozzle. The orifice diameter of the nozzle is 0.8 mm, which is made of polyvinylidene fluoride (PVDF).

A high-speed camera and PDA were separately used to conduct spray visualization and simultaneous droplet size, velocity, and volume flux measurement, respectively. Figure 3 shows a diagram of the measurement.

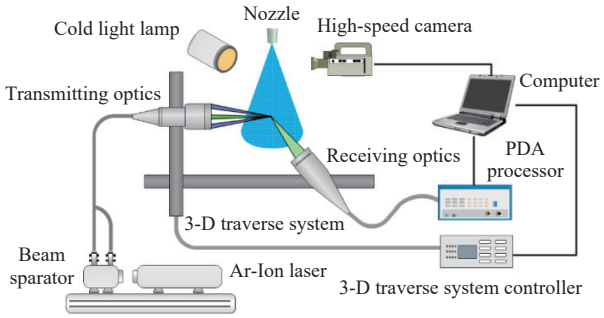

Figure 3 Schematic of the measurement

PDA is a single-point optical measuring technique that can measure the droplet parameters in the fluid in real-time without interrupting the fluid flow. The PDA system used in the research is a three-dimensional particle dynamic analyzer produced by Dantec Dynamic A/S. The system's key components are Argon-Ion laser, beam separator, transmitting optics, receiving optics, PDA processor, computer with BSA Flow software, three-dimensional traverse system, and controller. Table 1 lists the specifications of the PDA.

Table 1 Parameters of the PDA system

Parameters	Value
Power of laser/W	5
Focal length of transmitting optics/mm	800
Beam diameter/mm	2.2
Beam spacing/mm	74
Beam expander ratio	1.000
Type of receiving optics	112 mm Fiber PDA
Focal length of receiving optics/mm	800
Scattering angle/(°)	67
Scattering mechanism	Refraction

The beam separator split the monochromatic light from the laser into six beams in three different colors, green (514.5 nm), blue (488.0 nm), and violet (476.5 nm), were then sent to the transmitting optics. In this investigation, just two green beams (514.5 nm) and two blue beams (488.0 nm) were utilized, and they were focused on one spot, the measurement point. The receiving optics received the reflected laser beams and transferred them to the PDA processor, transforming the optical signal into an electrical signal. Finally, BSA Flow software processed the electrical impulses on the computer and produced the measurement results. Thanks to the three-dimensional traverse system, multiple points could be measured without optical alignment, which enabled the transmitting and receiving optics to move simultaneously. Moreover, the operation of the controller was also completed by the BSA Flow software.

The atomization characteristics of the pressure swirl nozzle were investigated by utilizing backlight photography technology to capture the image of the spray. A high-speed camera (PCO. Dimax cs4, with a pixel resolution of 2016×2016) and a cold light lamp were used in the photographic technology. The camera employed a zoom lens to capture high-quality photos of the liquid film (AF Zoom NIKKOR 24-85 mm f/2.8-4D). The camera with a zoom lens was placed in front of the nozzle, and the cold light lamp was placed behind it to give enough backlighting for the spray. The luminous efficiency of the cold light lamp (RF-400 Pro) was 155 lx/W, ensuring a stable and flicker-free image under high-speed photography at 100 000 fps. Using Image-Pro Plus software, the breakup length of the liquid film and the spray cone angle was calculated from the collected pictures.

2.2 Experimental measurement setup

This article studied the spray characteristics at the near-field spray of the pressure swirl nozzles at different Reynolds numbers, focusing on droplet size, velocity, and distribution. Images were recorded by PCO Dimax Camware 4 software at frame rates of 7600 fps (with an exposure time of 1.454 μs) for far-field and 12 742 fps (with an exposure time of 1.28 μs) for near-field, equivalent to the resolution of 624×688 and 600×700 pixels, respectively. The far-field images were for the observation of the entire spray, studying the liquid process from leaving the nozzle to the formation of droplets. The near-field images mainly captured the breakup characteristics of the liquid film. The investigation of the breakup length of the liquid film necessitated capturing more incredible details. The experiment changed the camera and lens settings to examine the transition from the liquid film to the ligament region. Therefore a 60 mm macro lens with F8 aperture was used.

For the measurement of droplet characteristics, we set the first measurement point to be 20 mm from the nozzle in the axial direction, and we set the step size to 10 mm. The step size in the radial direction was set to 2 mm and finally measured to the spray's edge. The setting of measurement points is shown in Figure 4. The point here is the measurement point. The PDA system sampled 3000 points at each measurement point or the measurement time was up to 30 s to complete the measurement. The experiment was carried out at the spray pressures of 0.2, 0.4, 0.6, 0.8, 1.0 MPa, with each experiment being performed three times to ensure the repeatability of the measurement statistics.

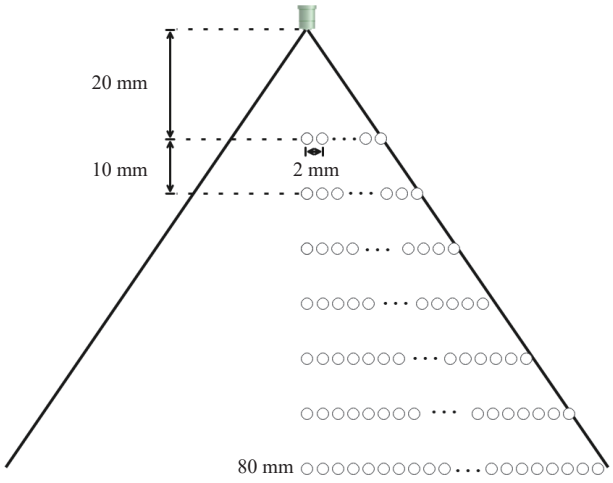

Figure 4 Measurement points setting

Measurements were taken throughout the spray to completely describe the flow and understand the spray dynamics for the pressure swirl nozzles, and the findings were presented in terms of Reynolds number. Reynolds number is the ratio of fluid inertial force to viscous force, which is a dimensionless number used to

categorize the fluid systems. Mathematically, Reynolds number is defined as following equation[17]:

$$\mathrm{Re}_p = \frac{\rho_l v D}{\mu_l} \tag{1}$$

With the liquid flow generated by the pressure swirl nozzle, Bernoulli's equation becomes[18]

$$p_1 = p_2 + \frac{1}{2}\rho_l v^2 \tag{2}$$

With $\Delta P = p_1 - p_2$, v becomes

$$v = \sqrt{\frac{2\Delta P}{\rho_l}} \tag{3}$$

$$\mathrm{Re}_p = \frac{\rho_l D}{\mu_l}\sqrt{\frac{2\Delta P}{\rho_l}} \tag{4}$$

where, v is the liquid film velocity based on pressure differential, m/s. ΔP is the pressure differential, Pa. μ_l is the liquid viscosity, Pa·s. ρ_l is the liquid density, kg/m^3, and D is the nozzle orifice diameter, m.

Table 2 lists the calculation results of Reynolds number and the flow rate at different pressures.

Table 2 Reynolds number and flow rate at different spray pressures

Pressure/MPa	Reynold number	Flow rate/L·h^{-1}
0.2	5369	54.024
0.4	7593	60.084
0.6	9300	83.205
0.8	10 738	99.377
1.0	12 006	112.993

2.3 Measurement parameters

The droplet size and velocity in the spray are the main physical parameters of the essential spray properties. Moreover, the average diameter is used to describe the spray quality and droplet size. SMD stands for Sauter average diameter, which is defined as the ratio of the total liquid volume to the total droplet surface area[19], shown as Equation (5):

$$\mathrm{SMD} = \frac{\sum_{i=1}^{N} D_i^3}{\sum_{i=1}^{N} D_i^2} \tag{5}$$

where, D_i is the diameter of the droplets, m; and N is the total number of the droplets.

In addition, as the average volume diameter D_{30} is also often used to describe the size of the droplets in the spray[5].

$$D_{30} = \left(\frac{\sum_{i=1}^{N} D_i^3}{N}\right)^{\frac{1}{3}} \tag{6}$$

The relative span factor (*RSF*) evaluates the dispersion of droplet size and spray uniformity. *RSF* is a dimensionless parameter calculated as:

$$RSF = \frac{D_{V0.9} - D_{V0.1}}{D_{V0.5}} \tag{7}$$

where, $D_{V0.1}$, $D_{V0.5}$, $D_{V0.9}$ are the diameter at which, respectively, 10%, 50%, 90% of the volume of droplets are contained in droplets at or below the diameter. The spray will be more uniform if the *RSF* value is near 1[20].

Different colored lasers were used to detect droplet velocity in different directions. The green light measured the axial velocity and the blue light measured the radial velocity in this experiment. In addition, the fluctuations of the root mean square (RMS) values of the two velocity components were also discussed in the study of the process of atomization.

The volume flux (cm^3/cm^2·s) is a vector that represents the liquid volume (cm^3) that flows through a probe area (cm^2) normal to the flow velocity direction, per unit time (s). Bade and Schick compared the volume flux results obtained by mechanized measurement and phase Doppler interferometry (PDI) techniques, finding that the two measurement methods reached 97% agreement[21]. The calculation equation of volume flux is as follows:

$$VF = \frac{\frac{\pi}{6} D_{30}^3 N}{A_{PV} t_{total}} \tag{8}$$

where, A_{PV} is the cross-sectional area of the probe area, m^2; N is the total number of droplets. t_{total} is the total measurement time, s. D_{30} is measured by PDA; N and t_{total} are also the parameters recorded by PDA. A_{PV} is related to the beam diameter, beam expansion ratio, and beam spacing of the laser.

The spray cone angle is another essential element for determining atomization quality since it influences the spray coverage and dispersion in the application[22]. The angle between the two straight lines connecting the center of the nozzle orifice and the end of the straight line on the spray boundary, as illustrated in Figure 5, is used to calculate the spray cone angle in this study. The two lines in the figure represent the edges of the spray, and the angle between the two lines is the spray cone angle.

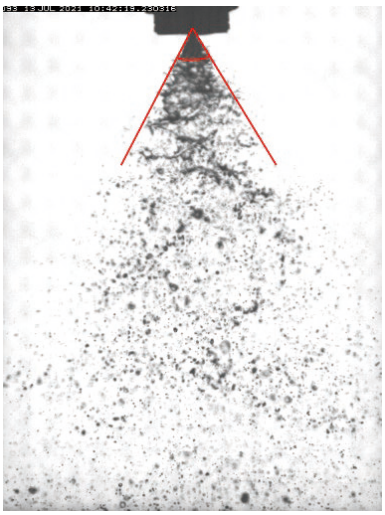

Figure 5 Schematic of spray cone angle measurement

3 Results and discussion

3.1 Breakup characteristics of full-cone pressure swirl nozzle

The atomization process of pressure swirl nozzles can be divided into two steps: primary breakup and secondary breakup. There are initial disturbances at the liquid - gas interface during the process of the primary breakup. Furthermore, the processes that allow these disturbances to proliferate will produce hydrodynamic instabilities and relatively large drag forces in the liquid film emerging from the nozzle, causing the liquid film to break up into ligaments or other irregular liquid elements. The aerodynamic instabilities lead larger droplets to distort and break up into smaller daughter droplets, resulting in a secondary breakup regime. Based on the aforementioned analysis, this article divided the spray of a pressure swirl nozzle into three regions, as shown in Figure 6. The

first is the liquid film region, where it is produced by the liquid leaving the nozzle after pressure swirling. Following the breakup of the liquid film, the ligament region is formed, which consists of the ligaments and other irregular liquid elements. The ligaments break into the droplets during the secondary breakup, called the droplet region.

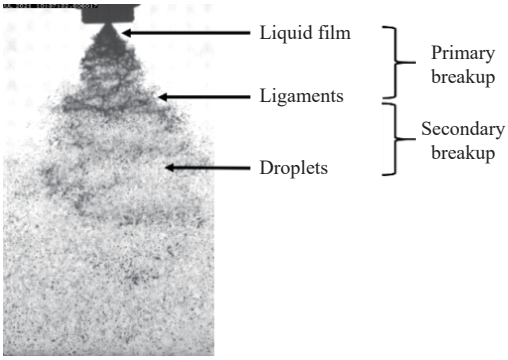

Figure 6 Representative spray profile for pressure swirl nozzle

The Reynolds number influenced the spray profile of the pressure swirl nozzle. It could be observed that the liquid film did not break up immediately, but burrs formed on the surface of the liquid film. This is because the surface wave at the liquid film had a tiny amplitude. However, when the wave traveled a certain distance in space and the amplitude reached its maximum, the liquid film would be sheared off into ligaments. The development of time will have little effect on the surface wave at a specific spatial location. As a result, for the linear stability theory, commonly used to solve surface waves, the spatial model was better suited for actual application, such as determining the liquid film breakup length[23].

Figure 7 depicts atomization images captured by the high-speed camera at various Reynolds numbers. The images were taken with a high-speed camera with a resolution of 624×688 pixels using the shadowgraph method, with an exposure time of 1.454 μs and a frame rate of 7600 fps. The liquid film was produced after the liquid exited the nozzle, as indicated in Figure 7. The liquid film progressively broke down into ligaments and droplet clusters, which eventually into droplets as the spray developed.

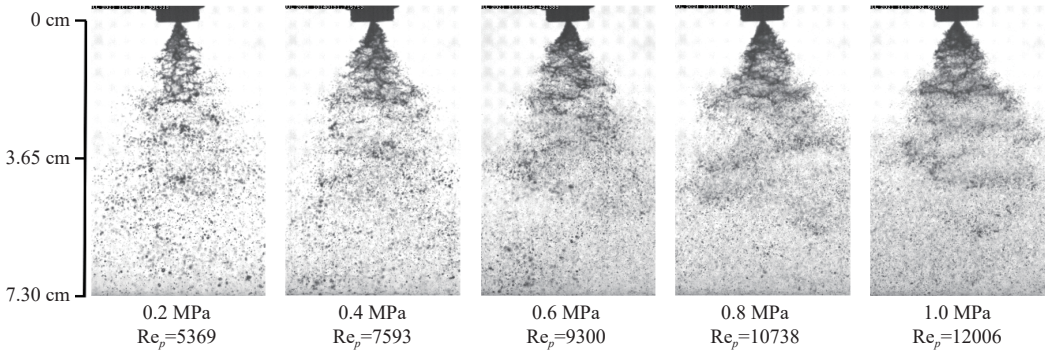

Figure 7 Pictures of atomization at different Reynold numbers

The spray became denser near the nozzle as the Reynolds number increased, as shown in Figure 8. The red circle in the figure is the location where the liquid film is broken. However, the spray appeared more transparent when compared to images with low Reynolds numbers. According to the flow rate data in Table 1, the higher the Reynolds number, the higher the flow rate, which implied that more spray liquid exited the nozzle, resulting in dense spray near the nozzle.

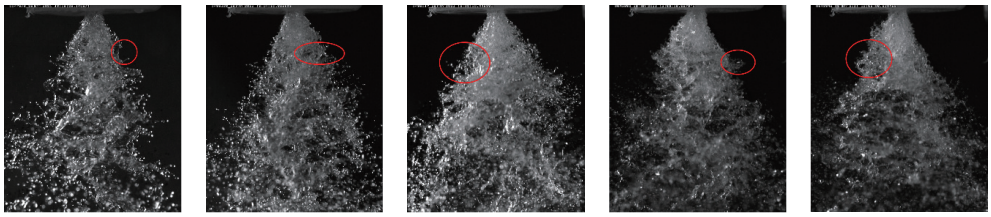

Figure 8 Pictures of the liquid film at different Reynold numbers

According to the above-mentioned judgment based on the breakup length of the liquid film and the experimental images (Figure 8), it can be concluded that there are three situations in which the liquid film breaks up: 1) “Gap” appeared at the breakage of the liquid film, that is, the surface wave broke at the wave hollow (Figures 8a and 8b); 2) “Burrs” appeared at the breakage of the liquid film, that is, the surface wave broke at the wave crest (Figure 8d); 3) Tearing occurred at the fractured liquid film, and bubbles appeared in the original continuous liquid film, as shown in Figures 8c and 8e.

According to the above situation, the broken images of liquid film at various Reynolds numbers were processed and measured, and the results were obtained.

Figure 9 depicts the breakup length and spray cone angle measurements at various Reynolds numbers. The breakup length reduces as the Reynolds number rises, but the spray cone angle rises. The spray liquid had a low viscosity due to the high Reynolds number so that the liquid in the swirl chamber was not easy to overflow. In addition to this, when Reynolds number increased, the swirl strength of the pressure swirl nozzle grew, and the liquid leaving the nozzle had a higher axial velocity, so the liquid film had a greater tendency to disintegrate earlier. The electrode of the electrostatic nozzle with induction charging acted on the region where the liquid film breakup. As a result, the position of the electrode can be determined by the visualization of liquid film breakup at various Reynolds numbers, enhancing the charging

efficiency and reducing electrode material usage.

However, because of the increased swirl strength, the increased friction of the spray liquid in the nozzle lowered the radial velocity. Hence, the liquid film near the nozzle outlet had a greater chance of spreading outward, resulting in the broader spray cone angle. The spray cone angle represented the range of the spray in certain senses. The wider spray cone angle indicated that the spray may cover more targets, which had implications for the spray range of the pesticide application.

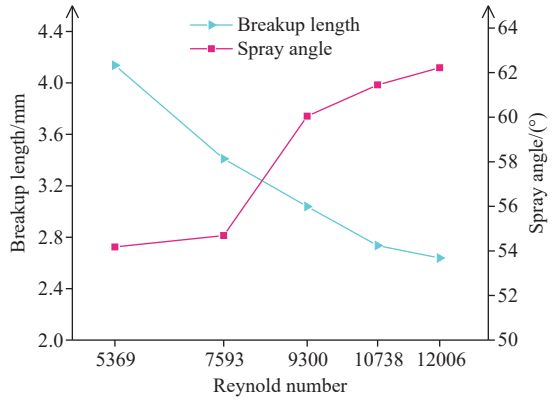

Figure 9 Effects of Reynolds number on breakup length and spray angle

The ligaments further disintegrate into droplets via Rayleigh capillary instability[24], as shown in Figure 8. There were specific differences in the atomization of the nozzle at different Reynolds numbers. The degree of atomization was evident in the droplet region at higher Reynolds numbers, and the droplets in this region were dense. However, for the low Reynolds number, there were primarily large droplets or droplet clusters at the droplet region after the breakup of the ligaments. This indicated that the droplets have not been atomized completely, resulting in a lower droplet density than the spray with a higher Reynolds number.

On the one hand, low viscosity made it simpler to break up ligaments into droplets for a high Reynolds number spray. On the other hand, the increase of swirl strength accelerated the fragmentation of the ligaments and droplet clusters, improving the atomization of the pressure swirl nozzle. It was also illustrated by the difference in the liquid film region and ligament region at various Reynolds numbers (Figure 8). The length between the nozzle tip and the droplet region was measured to evaluate the droplet characteristics of the droplet region at different Reynolds numbers, identifying the droplet characteristics research range. According to the measurement results, the droplet region appeared at a distance of approximately 2 cm from the nozzle.

3.2 Droplet size characteristics of full-cone pressure swirl nozzle

Although the nozzle is a full-cone pressure swirl nozzle, as the Reynolds number increases, the spray at the near-field of nozzle will become challenging to maintain an accurate full-cone spray, and the spray will become hollow[4]. In this measurement, the data rate of droplets at the center core of the spray is relatively low, especially at the high Reynolds number. The swirling component of the liquid in a pressure swirl nozzle helped spread the droplets toward the outer periphery, and the higher Reynolds number leads to the greater centrifugal force[25]. As the Reynolds number increased, the spray cone angle increased, explaining why the liquid flows outwards and the interior became empty, finally producing an air core inside the spray. Hence these measurement points will be ignored in the following analysis.

Variation in SMD with the axial and radial location at various Reynolds numbers is shown in Figure 10. The size of the green bubble in the figure represents the SMD of each measurement point. Larger droplets appeared near the center core of the spray and the ligament region. This phenomenon was evident for the spray at lower Reynolds numbers. For Re_p = 5369 and Re_p = 7593, the SMD of droplets near the center core of the spray decreased slightly trend with radial direction, suggesting the presence of droplet deformation and breakup. However, this trend at higher Reynolds numbers was not noticeable because the unstable and large droplets formed through the breakup of the ligaments at lower Reynolds numbers. Furthermore, these droplets experienced the secondary atomization generating smaller and more stable droplets in the radial direction due to centrifugal and shear instabilities. On the contrary, with higher momentum and adequate atomization, the droplets formed by the ligaments were more stable and smaller at higher Reynolds numbers.

According to the preceding explanation, the centrifugal action created an air core near the centerline, and the range of the air core expanded as Reynolds numbers increased. Moreover, the droplets formed by the ligaments were distributed outside the air core because of the centrifugal effect. Analyzed in the radial direction, SMD exhibited an increasing tendency at different Reynolds numbers. At a relative radial position close to the air core, the diameter of droplets was tiny and uniform. And the increasing tendency of the radial position near the air core is not apparent. When the Reynolds number was 10 738, and the axial location was 70 mm, SMD nearly remained between 45 μm and 57 μm while the radial location increased from 22 to 40 mm. SMD quickly increased beyond the radial position of 40 mm, reaching between 70-110 m. This trend illustrated that the centrifugal effect of pressure swirls caused the heavier droplets to be carried to the periphery of the spray while the lighter droplets remain inside the spray.

We analyzed droplet size's probability density function (PDF) to learn more about the relationship between droplet size and radial position. Figure 11 shows the PDF with different radial locations of 30, 40, 50, 60, 70 mm at Re_p = 12006. As reported by the research of Shrigondekar et al.[20] on full-cone pressure swirl nozzles with X-shaped blades, the droplet size distributions satisfied the log-normal distribution, which was given by Equation (9):

$$f_N(D) = \frac{1}{\sqrt{2\pi}D(\ln\sigma_{LN})} e^{-\frac{1}{2}\left[\frac{\ln(D)-\ln(\bar{D})}{\ln\sigma_{LN}}\right]^2} \quad (9)$$

where, D is the droplet diameter, m; $\bar{D}$ is the logarithmic mean size of distribution, m; σ_{LN} is the width of the log-normal distribution (dimensionless).

The study analyzed the axial location of 80 mm, which had a steadier spray than the area near the nozzle. It can be observed that the droplet diameter exhibited a bimodal distribution, with the second peak appearing on larger diameter values based on the log-normal distribution, indicating the secondary breakup (Figure 11). With the radial direction, the diameter value corresponding to the second peak of the PDF moved to a higher value. At the radial locations of 30 mm and 40 mm, the value of the first peak was greater than the second peak, which meant that the population of the finer droplets (droplet diameter of about 20 μm) occupied the majority at these positions. Nevertheless, with the centrifugal effect of pressure swirls, the finer droplets began to coalesce, resulting in the appearance of the second peak.

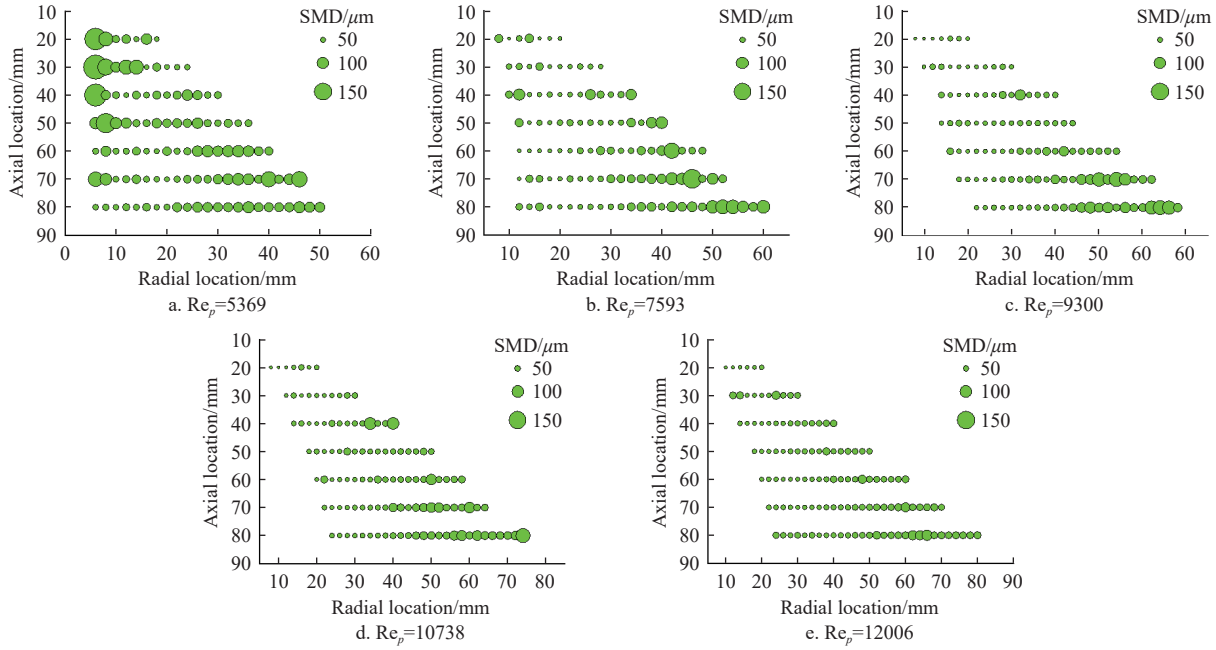

Figure 10 Variation in SMD with the axial and radial location at various Reynolds numbers

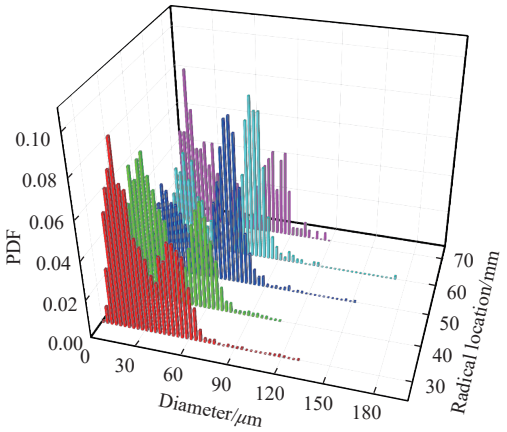

Figure 11 PDF of various radial locations at Rep = 12 006 with the axial location of 80 mm

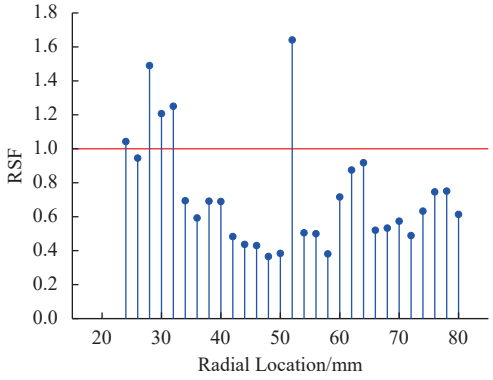

Figure 12 RSF of various radial locations at Rep = 12 006 with the axial location of 80 mm

Furthermore, the flow rate affected the population of droplets after the breakup of the ligaments as a result of the higher coalescence probability. The value of the second peak grew as the radial location approached 60 mm, whereas the value of the first peak steadily declined. The increase in the radial distance will lead to a more substantial centrifugal effect and a higher coalescence probability of the fine droplets. As the radial distance increases further, the droplets will eventually contact outside airflow, which will suffer a more significant drag force. Therefore, the diameter of large droplets decreased at the outer periphery of the spray due to the second droplet deformation. With the radial location of 70 mm, it was evident that the proportion of tiny droplets started to increase, while the proportion of large droplets decreased.

The *RSF* measured in the spray along the radial direction under the Re$_p$ = 12 006, axial location = 80 mm, is shown in Figure 12. The *RSF* is an excellent way to characterize the homogeneity of the spray. The droplets had high homogeneity when the radial distance was less than 30 mm, and the *RSF* was about 1. However, the region with droplet coalescence, where the radial location was between 30 mm and 60 mm, shows poor uniformity. This trend indicated that the droplet coalescence had a particular effect on the *RSF*. At the outer periphery of the spray, the uniformity of droplets improved since the drag force broke the droplets.

3.3 Droplet velocity characteristics of full-cone pressure swirl nozzle

At varying Reynolds numbers, the velocity fields in the axial cross-section are shown in Figure 13. As the Reynolds number grew from 5369 to 12 006, the magnitude of the average droplet velocity increased from 3.045 m/s to 3.330 m/s. This indicated that the increase of Reynolds number helped promoting the pressure swirls, causing higher momentum of droplets. From the description of droplet size above, the droplet size was finer at the higher Reynolds number. Compared to the larger droplets, finer droplets were more prone to gaining higher momentum due to stronger pressure swirls, resulting in a higher maximum value of droplet mean velocity.

Variations in droplet size and average droplet velocity changing in the radial direction, were highly significant in analyzing the spray velocity field (Figure 14). The mean velocity of droplets at various Reynolds numbers decreased with the radial direction (Figure 13). Analyzing the droplet size under the same conditions, it was clear that the droplets near the air core inside the spray were finer and more susceptible to centrifugal action. So, the droplets inside the spray had a greater average velocity. On the contrary, the droplets outside the spray had a greater diameter due to coalescence. On the one hand, the droplets' coalescence meant that there were many collisions between the droplets. The collision caused the droplets to lose kinetic energy, which led to a decrease in the average velocity.

On the other hand, big droplets had a large surface area and a larger area in contact with the outer air when moving, which experienced greater drag force so that the mean velocity of the periphery was lower than the mean velocity inside the spray.

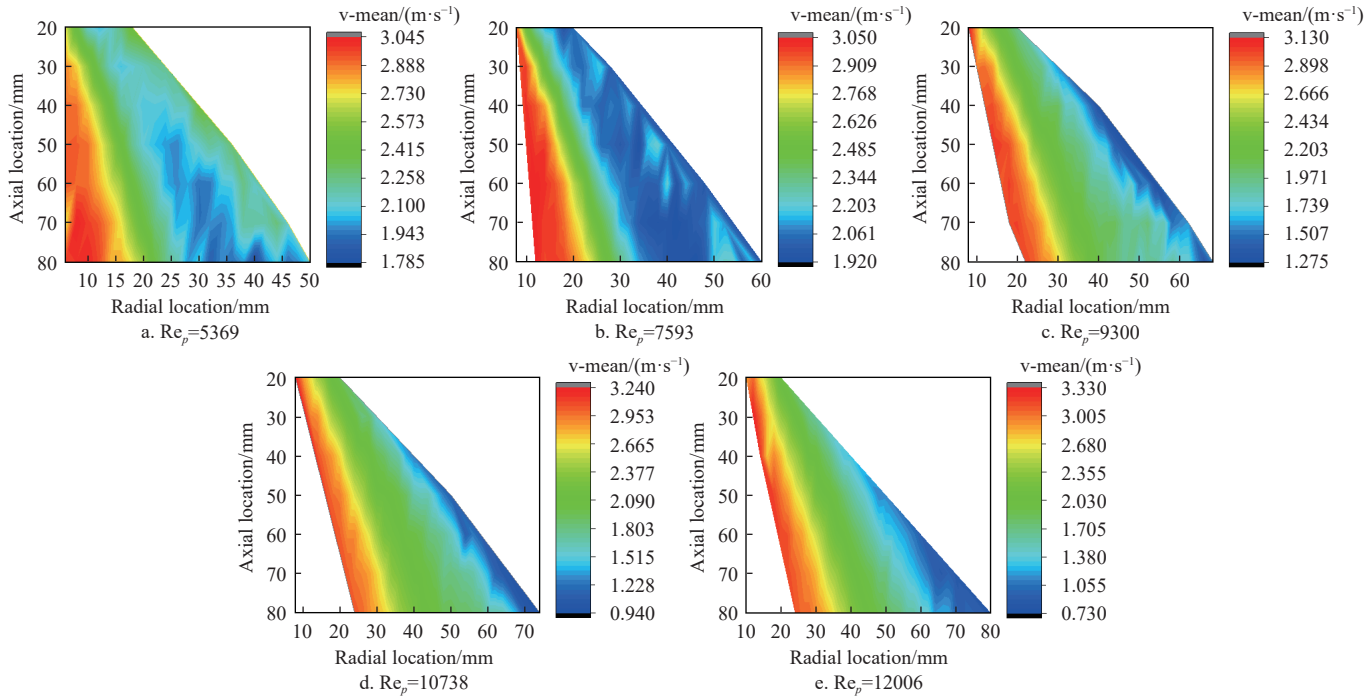

Figure 13 Velocity fields in the axial cross-section at different Reynolds numbers

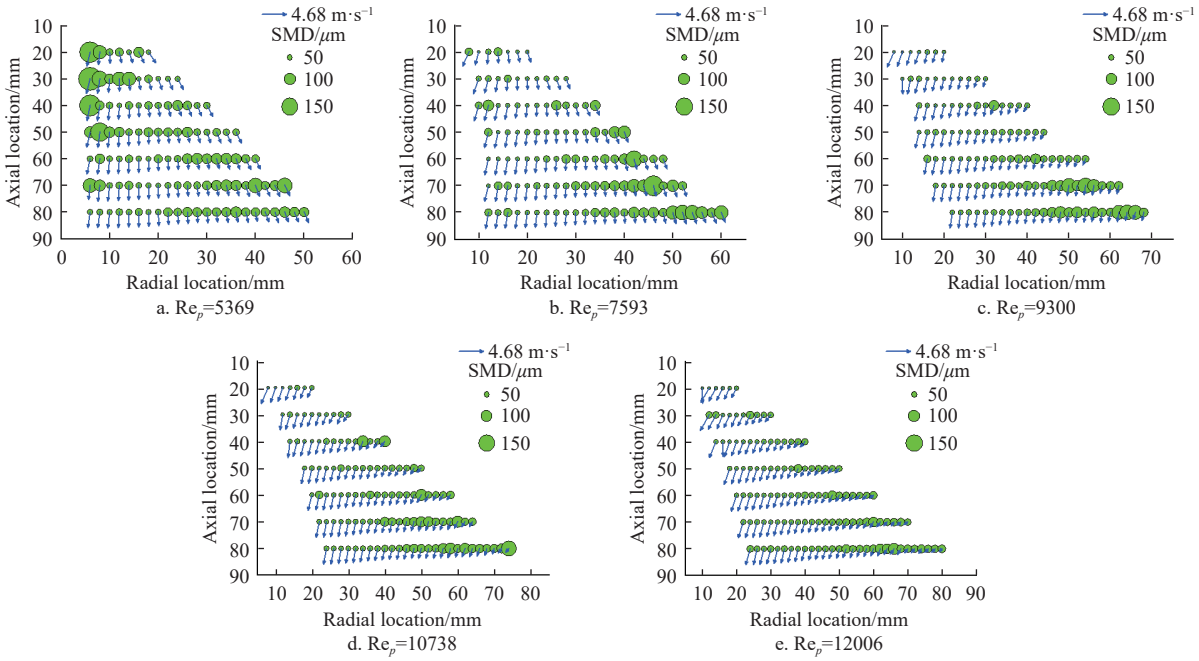

Figure 14 SMD and average velocity vector along with the axial and radial distance at different Reynolds numbers

The direction of the droplet average velocity vector had also changed with the Reynolds number (Figure 14). The size of the green bubble in the figure represented the SMD of each measurement point, and the direction of the arrow at each position indicated the direction of the average velocity, and the length of the arrow indicated the size of the average velocity. The velocity direction of the droplets away from the spray center axis was outward when the Reynolds numbers are 5369 and 7593. However, the average droplet velocity gradually inverted as the Reynolds number rises. From the aforementioned study, the velocity decreased with the increase of the radial distance. As indicated in Equation (10), this was related to the centripetal force experienced by the droplets in the pressure swirl spray.

$$F = \frac{mv^2}{r} \tag{10}$$

where, F is the centripetal force experienced by the droplet, N; m is the mass of the droplet, kg; v is the tangential velocity of the droplet, m/s; and r is the radial distance of the droplet, m.

At a low Reynolds number, the kinetic energy of the droplets after leaving the nozzle was relatively small, resulting in the

centripetal force was not enough to continue the swirling motion, so the droplets located on the periphery of the spray began to spread outward. It can be seen that the increase in Reynolds number made the droplets obtain greater kinetic energy (Figure 13). Although the collision of the droplets reduced the kinetic energy, the mass of the droplets was also increasing due to the coalescence, so the velocity direction was inwards. This showed that the increase of Reynolds number promotes the atomization of the pressure swirl nozzle in some ways so that it can maintain the swirl motion better.

The study also analyzed the RMS value of axial and radial velocity and the radial distance at different Reynolds numbers (Figure 15). The RMS of the axial velocity component (Velocity U-RMS) had a small RMS value near the spray core, and velocity U-RMS tended to increase slightly as the radial distance increased. However, from the perspective of velocity U-RMS fluctuations, velocity U-RMS does not vary significantly, remaining essentially constant at 1. In addition, Reynolds number also had little effect on the fluctuation of velocity U-RMS, which meant that the axial velocity component was mainly affected by gravity, and hence will not experience substantial changes causing by droplets breakup, or coalescence.

The tendency of RMS of radial velocity component (Velocity V-RMS) is opposite to the velocity U-RMS. The tiny droplets located in the center region of the spray had a larger velocity V-RMS, while large droplets far from the center region had fewer fluctuations of velocity U-RMS. The explanation for this might be that tiny droplets are more prone to be affected by the pressure swirls, while the large droplets had a limited response to the fluctuations[26]. What's more, the velocity V-RMS was significantly affected by the Reynolds number. It can be seen from Figure 15 that when the Reynolds number was 5369, the velocity V-RMS fluctuation from the center of the spray to the periphery of the spray was about 1. On the contrary, as the Reynolds number rises to 12 006, the variance decreased to around 20. The results demonstrated that Reynolds number also affected the flow of the spray, activating the droplets of the spray, which led to an increase in the fluctuation of velocity V-RMS.

3.4 Liquid volume flux of full-cone pressure swirl nozzle

The values of liquid volume flux measured in both the radial and axial direction for various Reynolds numbers is shown in Figure 16. The abscissa and ordinate here represented the axial and radial locations respectively, and the curve at every axial location was drawn from the volume flux values calculated from measurement points at different radial locations. In this paper, the volume flux curve varying with radial distance was plotted in the exact figure under the same Reynolds number and different axial distances. The dashed line under each axial distance represented that the volume flux is 0. The figure can depict the distribution of the liquid volume flux.

With the increase of Reynolds number, the volume flux gradually diffused in the radial direction as the axial distance increased. When the Reynolds number increased from 5369 to 12 006, the maximum radial diffusion range of the volume flux with an axial distance of 80 mm rose from 45 mm to 80 mm. Furthermore, the liquid volume flux with a radial distance of less than 20 mm gradually decreased as the increase of Reynolds number, resulting in more and more hollowness in the center region of the spray. From the above analysis of droplet size and velocity, the droplets were mostly tiny with low velocity when the Reynolds number was low. The increase in Reynolds number meant that the spray liquid had a higher swirl strength, resulting in the droplets with greater momentum. The centrifugal effect was conducive to the acceleration of tiny droplets and their outward movement, which increased the probability of droplets' coalescence at the same time. These factors led to the diffusion of the liquid volume flux with the increase of the Reynolds number. This effect may also be seen in the spray cone angle, which increased as the Reynolds number increases. It can be known from the change in volume flux that an appropriate increase in Reynolds number can increase the spray range and the coalescence and acceleration of the droplets, improving the deposition of droplets on the target.

It can be observed that the liquid volume flux gradually increased along the axial direction. From the velocity analysis above, although the axial velocity of the droplet fluctuated slightly, the axial velocity component mostly impacted by gravity dominates the spray flow field, causing the volume flux to rise as the distance increases. Analyzing from the radial distance, the volume flux along the radial direction, beginning at the central axis of the spray, gradually grew to its maximum first and then gradually decreased. It was because of the size of the small droplets near the spray air core. With the development of the spray, the centrifugal effect helped the small droplets move gradually outwards, increasing the probability of droplets collision and coalescence, so the liquid volume flux increased. However, when the droplet size grew larger, the drag force slowed down the further diffusion of the droplet, resulting in a reduction in volume flux. In general, the development of the spray made the liquid volume on the spray section in the axial direction more uniform. The analysis of liquid volume flux provided the apparent distribution of liquid at the near-field of the nozzle, which may be used as a reference for electrostatic nozzle electrode design and spray distance selection.

4 Conclusions

This article investigated the near-field atomization properties of a full-cone pressure swirl nozzle at various Reynolds numbers. The high-speed camera was used to research and analyze the spray breaking visually. At the same time, the particle size, velocity, and volume flux of the spray droplets were measured from the axial and radial directions using PDA. The results of the study are as follows.

According to the results of the high-speed camera, this paper divides the spray produced by the full-cone pressure swirl nozzle into three regions, the liquid film region, the ligament region, and the droplet region. The breaking length of the liquid film of the solid cone pressure swirl nozzle is related to the Reynolds number. The Reynolds number influences the flow of liquid in the pressure swirl nozzle, i.e., the swirl strength and the stability of the liquid film created after the liquid exits the nozzle are related to this. The higher the Reynolds number, the more unstable the liquid film is, leading to the shorter breakup length of the liquid film. In addition, the spray cone angle is also affected by the change in swirl strength caused by the Reynolds number.

In order to create a clear description of the spray characteristics of the full-cone pressure swirl nozzle at the near-field of the nozzle, this article examines the three parameters of droplet size, velocity, and volume flux in the droplet region. It can be observed that large droplets appear in some areas with a low degree of atomization, such as the proximal ligament area, the area near the central spray axis, and the area with a relatively low Reynolds number. In the radial direction, the droplet size tends to increase. The droplet size distribution function shows that the coalescence of droplets happens along the radial direction due to the centrifugal force, increasing the droplet size. In the case of a large Reynolds number, the droplets

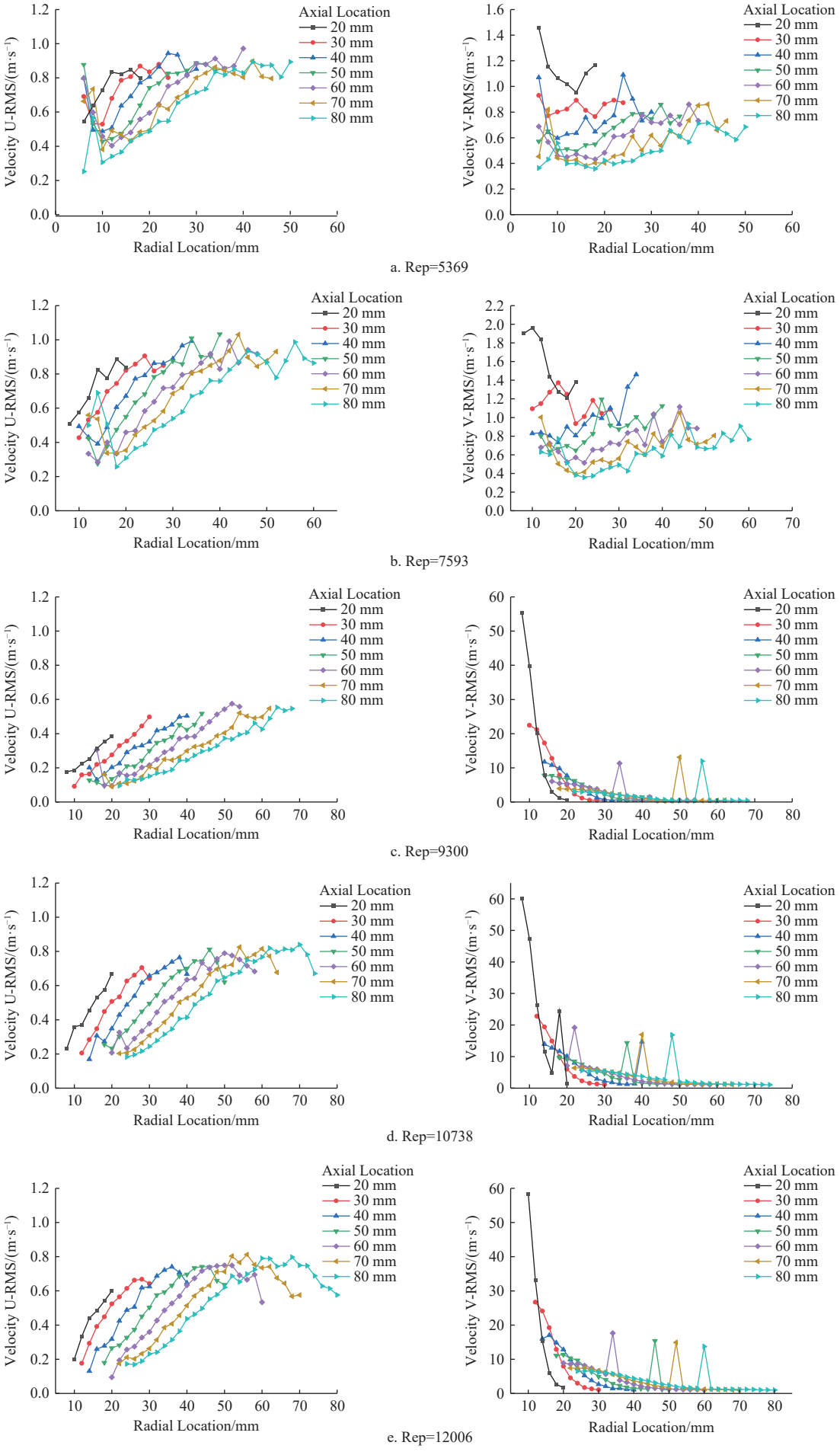

Figure 15 RMS value of axial and radial velocity along with the radial distance at different Reynolds numbers

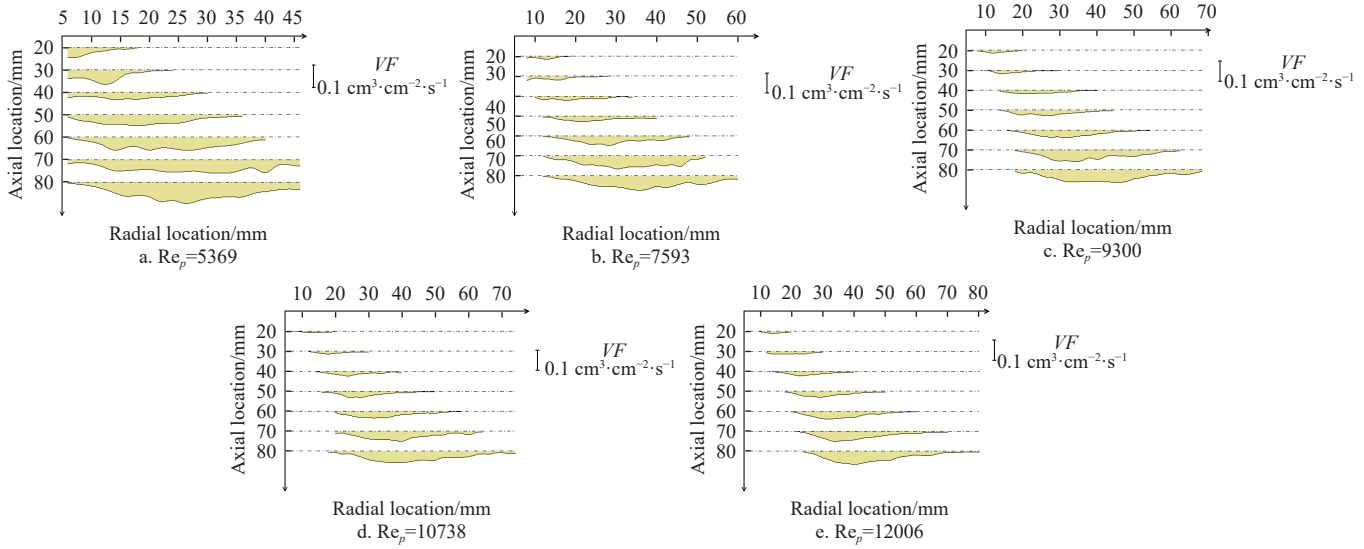

Figure 16 Liquid volume flux measured along the radial and axial direction under various Reynolds number

will have greater momentum during the spraying process. The average velocity of droplets with smaller particle sizes near the spray center axis is high, and these small droplets are more susceptible to the influence of the airflow and produce larger velocity fluctuations. Because the droplets are mainly impacted by gravity, the average droplet velocity in the axial direction has little change, and the fluctuation is slight. The liquid volume flux distribution shows the liquid distribution of the spray in the droplet region. It can be observed that with the increase of Reynolds number, the spreading range of spray expands. However, due to the large axial velocity, the volume flux increases with the axial distance. The liquid volume flux will increase to a maximum in the radial direction and then decrease, related to the droplet size inside the spray.

This article focuses on three factors relevant to applications when studying the spray of a full-cone pressure swirl nozzle: droplet size, velocity, and volume flux. The droplet size and velocity characteristics influence the trajectory of the droplet in the air, and in turn, its deposition on the crop target. The volume flux distribution represents the volume distribution at each position of the droplet region, and to a degree, depicts the quantity of spray at each position. Evaluating the droplet size, velocity, and volume flux may offer a definite reference for the selection of operating parameters such as spray distance and Reynolds number, thereby reducing droplet drift loss and boosting operating efficiency. On the one hand, the application of breakup characteristics in agricultural nozzles is that the deformation of liquid affects the following production of droplets, therefore affecting droplet deposition. On the other hand, the broken area of the liquid film is the principal action position of the agricultural induction electrostatic nozzle. As a result, the location of the electrode may be reliably established by observing the breakup characteristics and measuring the breakup length of the liquid film, providing a certain reference for the design of the electrostatic nozzle.

Acknowledgements

The authors wish to acknowledge the support provided by National Natural Science Foundation of China (Grant No. 31971797), National Natural Science Foundation of China (Grant No. 32271997), China Agriculture Research System of MOF and MARA (CARS-26), General Program of Guang-dong Natural Science Foundation (2021A1515010923), Guangdong Provincial Special Fund For Modern Agriculture Industry Technology Innovation Teams (Grant No. 2023KJ108) and Key-Area Research and Development Program of Guangdong Province (2023B 0202090001).

[References]

[1] Laryea G N, No S. Development of electrostatic pressure-swirl nozzle for agricultural applications. Journal of Electrostatics, 2003; 57(2): 129–42.

[2] Belhadef A, Vallet A, Amielh M, Anselmet F. Pressure-swirl atomization: Modeling and experimental approaches. International Journal of Multiphase Flow, 2012; 39: 13–20.

[3] Santolaya J L, Aísa L A, Calvo E, García I, García JA. Analysis by droplet size classes of the liquid flow structure in a pressure swirl hollow cone spray. Chemical Engineering and Processing:Process Intensification, 2010; 49(1): 125–131.

[4] Hamid AHA, Atan R. Spray characteristics of jet–swirl nozzles for thrust chamber injector. Aerospace Science and Technology, 2009; 13(4-5): 192–196.

[5] Sun Y, Alkhedhair A M, Guan Z, Hooman K. Numerical and experimental study on the spray characteristics of full-cone pressure swirl atomizers. Energy, 2018; 160: 678–692.

[6] Hewitt A J. Spray drift: impact of requirements to protect the environment. Crop Protection, 2000; 19(8): 623–627.

[7] Hilz E, Vermeer A W P, Cohen Stuart M A, Leermakers F A M. Mechanism of perforation based on spreading properties of emulsified oils. Atomization and Sprays, 2012; 22(12): 1053–1075.

[8] Makhnenko I, Alonzi E R, Fredericks S A, Colby C M, Dutcher C S. A review of liquid sheet breakup: Perspectives from agricultural sprays. Journal of Aerosol Science, 2021; 157: 105805.

[9] Durdina L, Jedelsky J, Jicha M. Investigation and comparison of spray characteristics of pressure-swirl atomizers for a small-sized aircraft turbine engine. International Journal of Heat and Mass Transfer, 2014; 78: 892–900.

[10] Zhang T, Dong B, Chen X, Qiu Z, Jiang R, Li W. Spray characteristics of pressure-swirl nozzles at different nozzle diameters. Applied Thermal Engineering, 2017; 121: 984–991.

[11] Santolaya JL, Aísa L A, Calvo E, García I, Cerecedo L M. Experimental study of near-field flow structure in hollow cone pressure swirl sprays. Journal of Propulsion and Power, 2007; 23(2): 382–389.

[12] Patel M K, Kundu M, Sahoo H K, Nayak M K. Enhanced performance of an air-assisted electrostatic nozzle: Role of electrode material and its dimensional considerations in spray charging. Engineering in Agriculture, Environment and Food, 2016; 9(4): 332–338.

[13] Senecal P K, Schmidt D P, Nouar I, Rutland C J, Reitz R D, Corradini M L. Modeling high-speed viscous liquid sheet atomization. International Journal of Multiphase Flow, 1999; 25(6): 1073–1097.

[14] Saha A, Lee J D, Basu S, Kumar R. Breakup and coalescence characteristics of a hollow cone swirling spray. Physics of Fluids, 2012;

24(12): 124103.

[15] Davanlou A, Lee J D, Basu S, Kumar R. Effect of viscosity and surface tension on breakup and coalescence of bicomponent sprays. Chemical Engineering Science, 2015; 131: 243–255.

[16] Song S R, Sun D Z, Xue X Y, Dai Q F, Li Z, Li Z, et al. Design of pipeline constant pressure spraying equipment and facility in mountainous region orangery. IFAC-Papersonline, 2018; 51(17): 495–502.

[17] Walzel P. Spraying and atomizing of liquids. Ullmann's Encyclopedia of Industrial Chemistry, 2000; pp.1-30. doi: 10.1002/14356007.b02_06.pub3.

[18] Wilson C. Chin. Managed pressure drilling. Elsevier, 2012.

[19] Lefebvre A H, McDonell V G. Atomization and sprays: CRC press; 2017. doi: 10.1201/9781315120911

[20] Shrigondekar H, Chowdhury A, Prabhu S V. Characterization of solid-cone simplex mist nozzles. Fire Safety Journal, 2020; 111: 102936.

[21] Bade K M, Schick R J. Phase Doppler Interferometry volume flux sensitivity to parametric settings and droplet trajectory. Atomization and sprays, 2011; 21(7): 537–51.

[22] Datta A, Som S K. Numerical prediction of air core diameter, coefficient of discharge and spray cone angle of a swirl spray pressure nozzle. International Journal of Heat and Fluid Flow, 2000; 21(4): 412–419.

[23] Dombrowski N, Hooper P C. The effect of ambient density on drop formation in sprays. Chemical Engineering Science, 1962; 17(4): 291–305.

[24] Sivakumar D, Vankeswaram S K, Sakthikumar R, Raghunandan BN. Analysis on the atomization characteristics of aviation biofuel discharging from simplex swirl atomizer. International Journal of Multiphase Flow, 2015; 72: 88–96.

[25] Rezaei S, Vashahi F, Ryu G, Lee J. On the correlation of the primary breakup length with fuel temperature in pressure swirl nozzle. Fuel, 2019; 258: 116094.

[26] Xia Y, Alshehhi M, Hardalupas Y, Khezzar L. Spray characteristics of free air-on-water impinging jets. International Journal of Multiphase Flow, 2018; 100: 86–103.